Bull Earthquake Eng
DOI 10.1007/s10518-014-9662-5

ORIGINAL RESEARCH PAPER

# Combining active and passive multi-channel analysis of surface waves to improve reliability of $V_{S,30}$ estimation using standard equipment

**Francisco Humire · Esteban Sáez · Felipe Leyton · Gonzalo Yañez**

Received: 3 July 2013 / Accepted: 4 August 2014
© Springer Science+Business Media Dordrecht 2014

**Abstract** Surface wave methods are commonly used for seismic soil classification, however, their indirect nature implies a degree of uncertainty that needs to be described and constrained. To evaluate dispersive characteristics, we use active and passive sources, linear and circular arrays, and frequency-wavenumber analysis, spatial autocorrelation method and Roadside MASW analyses. We test the reliability of this approach in three different soil conditions of the Santiago basin (Chilean capital) using standard equipment. This methodology is compared with reliable results from high-energy active source and borehole information. To obtain a confident shear wave depth-profile with standard equipment, it is necessary to combine the dispersion curves obtained with low-energy active source, passive linear and circular arrays. Results obtained only through a passive linear test may not guarantee a reliable 30 m of exploration, especially when no high-traffic roads are present nearby. According to results obtained in the Santiago basin, we propose a methodology based on a combination of active and passive results.

**Keywords** Surface wave methods · Seismic soil classification · Multichannel analysis · Santiago typical soils

F. Humire · E. Sáez (✉)· G. Yañez
School of Engineering, Pontificia Universidad Católica de Chile, Av. Vicuña Mackenna 4860, Macul, Santiago, Chile
e-mail: esaez@ing.puc.cl

E. Sáez
Center for Integrated Natural Disaster Management CONICYT/FONDAP/15110017, Av.Vicuña Mackenna 4860, Macul, Santiago, Chile

F. Leyton
Centro Sismológico Nacional, Universidad de Chile, Blanco Encalada 2002, Santiago, Chile

Published online: 13 August 2014

## 1 Introduction

The shear wave velocity profile is a fundamental parameter to evaluate the dynamic response of a site (Tokimatsu 1997). In-hole tests are commonly used to evaluate this parameter, but the borehole required is not always available. There are several approaches to estimate the soil shear wave velocity profile through the analysis of surface wave propagation, but as with any geophysical-indirect method, there is an important degree of uncertainty that needs to be quantified and eventually reduced. It is important to note that these geophysical methodologies integrate a broader soil volume, and therefore are probably more representative of the seismic behavior of a site than local in-hole measurements.

Rayleigh waves are dispersive; the phase propagation velocities are a function of frequency (Okada 2003). Surface wave methods use this property to characterize soils because their dispersion properties depend on the stratigraphy, particularly in the shear wave velocity profile. The procedure includes three phases (Tokimatsu 1997; Foti 2000): (a) observation and recording of surface waves, (b) determination of dispersion curves, and (c) estimation of a shear wave velocity profile compatible with the observations through an inversion procedure.

The Spectral Analysis of Surface Waves (SASW) is one of the most well known surface wave methods and has been widely studied by different authors (Nazarian and Stokoe 1984; Sanchez-Salinero 1987). This method uses a pair of receivers to record a signal generated for an active controlled source aligned with the receivers, thus, data gathered from different spacing distances is required to build up the dispersion curve. Multi-channel methods simultaneously record the signal with multiple receivers, decreasing the execution time when compared to the SASW approach (Park et al. 1999). Seismic sources can be either active (i.e. sledgehammer or a weight drop, mechanical oscillators), or passive (Bonnefoy-Claudet et al. 2009). In comparison to active sources, ambient vibrations allow the inference of the properties of deeper layers, due to their low-frequency content. In this paper, we study the critical aspects of surface-waves multi-channel analysis and its application in the city of Santiago (Chile), specifically: (1) seismic source, (2) processing techniques, and (3) their application on three different soil classes. The objective is to develop a reliable methodology able to estimate a shear wave velocity profile for the initial depth of 30 m ($V_{S,30}$) using standard equipment, and using as a reference the results obtained with other reliable methods, such as: (a) high-energy active source, (b) borehole/down-hole. A similar study has been reported by Comina et al. (2011), focused on evaluating the accuracy and the uncertainty of estimating $V_{S,30}$ from dispersive empirical data generated by passive and/or active surface-wave tests. In this research, the goal is to provide some guidelines for the appropriate combination of methods (active and passive) to calculate a reliable $V_{S,30}$ estimation with standard equipment, able to be used in urban areas while avoiding the use of high energy active sources.

## 2 Multichannel analysis of surface waves

Surface wave methods can be classified according to the source of the surface waves recorded, which are either active or passive. Passive sources generally require a 2D array of geophones, because the predominant direction of propagation of each wavefront is unknown. A linear array could be used, but an overestimation of phase velocities is expected (Park and Miller 2008).

## 2.1 Analysis of dispersion curves

Multichannel methods allow a simultaneous analysis of multiple geophone records through a transformation from time and space domains to another domain that allows the identification of energy peaks, and thereby the dispersive characteristics of the studied site (Foti et al. 2001). For this purpose, there are different approaches; the most well known and most used are the frequency-wavenumber analysis (f-k) and the spatial autocorrelation method (SPAC) proposed by Aki (1957). Also, the MASW method, popularized by Park et al. (1999), has been broadly used in recent years, especially since one of its variants allows analyses of linear passive tests (Roadside MASW; Park and Miller 2008).

The active tests were analyzed by using the f-k analysis considering the direction of waves known; on the other hand, passive tests using a 2D array were analyzed using f-k and SPAC methods. These tools were implemented in the GEOPSY package software (Wathelet 2002–2011). Passive measurements using linear arrays were analyzed using an implementation of Roadside MASW method that considers only planar incident wavefronts.

The f-k analysis assumes a plane wave front crossing the array of receivers with certain frequencies and wavenumbers. Hence, each signal is delayed according to the array's geometry so the arrival time of the plane wave front in each receiver is the same. The total array response is the sum of all delayed signals. If the waves are traveling with the assumed wavenumber, the contribution of each receiver will be constructive; hence, the total array response will be large for a given wavenumber. This process is repeated for different frequencies and timeframes, thus an energy spectrum associated with an array response can be constructed, in which energy peaks can be recognized to determine the dispersion curve of the site.

The SPAC proposed by Aki (1957) assumes ambient vibrations are a stochastic process stationary in time and space, and composed mainly of surface waves. Hence, the method assumes a homogenous distribution of sources in the space around the array. The main advantage of the SPAC analysis over f-k analysis is that fewer receivers and smaller arrays are required (Okada 2003). Aki (1957) established a spatial autocorrelation coefficient between a pair of receivers, and then an azimuthal average is calculated, giving information about all waves propagating under the influence of the floor structure beneath the receiver array (Okada 2003). The autocorrelation coefficient is associated with the dispersive properties of the soil structure through the Bessel function of first kind and zero-order (known as autocorrelation curve). Bettig et al. (2001) introduced an improvement [Modified Spatial Autocorrelation Method (MSPAC)] with the aim of calculating the azimuthal average of paired receivers whose distances are not exactly the same (a typical problem in long arrays). Chávez-García et al. (2006) suggest that the SPAC analysis is not restricted to a 2D array, provided that the wavefield is a stationary process. Thus linear arrays can be used, which is very useful in urban areas.

Park et al. (1998) proposed a transformation similar to the f-k analysis, where all signals are delayed and summed for a selected phase velocity. It allows the construction of a velocity–frequency diagram which shows peaks when the assumed value matches the phase velocity of the wave. In principle, this method was proposed for active measurements, but Park and Miller (2008) extended this methodology to ambient vibration measurement using linear arrays alongside a road. The method adds up the energy associated with all possible azimuths to construct the velocity–frequency diagram, enabling the identification of the dispersion curve. These same authors indicated that this method produces an overestimation of phase velocities that could be very significant for long wavelengths (over 75 m in their study).

### 2.2 Inversion: neighborhood algorithm

The inversion must generate a model of horizontal soil layers with elastic properties compatible with field observation in terms of the dispersive characteristics (dispersion or autocorrelation curves). The neighborhood algorithm (NA), by Sambridge (1999), is a global optimization method that, unlike iterative methods, does not require an initial model and widely explores the space of parameters. The NA generates random initial models evenly homogeneous in the parameter space. With these models, it evaluates the mismatch of each one, and selects the best model to generate new random models close to them. The difference between the analytical model and empirical data (misfit) is evaluated, and the process is repeated until the misfit reaches the minimum value possible. Wathelet (2008) proposed an improvement to NA, allowing the introduction of conditions between parameters of models. This last improvement has been implemented in a version of the Geopsy package software used in this research. The misfit function is evaluated through Eq. (1), where, $x_{(r,i)}$ and $x_{(c,i)}$ are the values of the dispersion properties of field observation and the calculated model, respectively; $\sigma_i$ is the standard deviation associated with field observation and $n_F$ is the number of frequency samples (Wathelet 2005).

$$misfit = \sqrt{\sum_{i=1}^{n} \frac{(x_{(r,i)} - x_{(c,i)})^2}{\sigma_i n_F}} \tag{1}$$

According to different authors (Xia et al. 1999; Wathelet 2005), the shear wave velocity ($V_S$) profile is the most influential parameter on the inversion process. Because changes in density or Poisson ratio produce negligible effects in dispersion properties, we use the same range of values of these parameters for all layers. In the inversion process, Poisson ratio and density respectively vary between 0.2 to 0.5 and 1,700 to 2,100 kg/m$^3$. Any additional data ($V_S$ or layer thickness) was a variable for the inversion process. $V_P$ was explicitly linked to $V_S$ by the Poisson ratio.

## 3 Results for different Chilean soil classes in the Santiago metropolitan area

In this investigation, we used a GEODE-12 (Geometrics ®), connected to 12 geophones (4.5 Hz natural frequency), located at intervals of 5 m. The sources used in the active test were 100 kg weight 3 m-drop and an 18 pound sledgehammer. The spacing between the receivers and the source determines the range of frequencies where the dispersion curve is valid (Foti 2000); hence, tests were conducted with different spacing between the source and receivers to get as much information as possible. Since we have no control over the generated wavefield or its frequency range, the test must be repeated a number of times to ensure that reliable dispersion properties are obtained. In addition, to improve the results, we stacked the active signals to increase the signal-to-noise ratio. We used a linear array with 5 m spacing between receivers, and a circular array with 9.8 m to record ambient vibrations. Due to the fundamental assumption that passive methods consider ambient vibrations as a superposition of surface waves that propagate with random directions (Tokimatsu 1997), a longer time record is required (Wathelet 2005) for ambient noise record. The time record used was 16 min in all cases, with sampling at 62.5 Hz.

In order to study the application of a multichannel analysis of surfaces waves, we selected three characteristic soils of the Santiago basin (Table 1). Each one is composed of soils with distinctive geological and low-amplitude dynamic properties. The objective is to determine

**Table 1** Cases studied

| Case | Place | Predominant stratigraphy |
|---|---|---|
| 01 | Lampa (northern Santiago) | Clays, sandy silts, loose and dense sands, silty sands |
| 02 | Pudahuel (western Santiago) | Volcanic ashes (ignimbrite) |
| 03 | Macul (southern Santiago) | Gravels |

the shear wave velocity profile and the harmonic mean of velocities in the initial depth of 30 m ($V_{S,30}$) at each studied site. This parameter, $V_{S,30}$, is a parameter commonly used for seismic soil classification. The three cases studied in this research are placed in urban areas but far from high-traffic roads. In Fig. 1, the distance and orientation of the closest street to the linear array is indicated. For each case, the homogeneous distribution of passive sources is checked against the f-k analysis of the circular array. Figure 2 shows the distribution of energy in the $k_x - k_y$ wavenumber space for some frequencies where SPAC information will be used. For different timeframes selected in each case, different orientations of passive sources are identified. Hence, the homogeneous source distribution hypothesis of the SPAC method is reasonably satisfied.

In the following section, we compare the dispersion curves obtained with active and passive experiments, using different arrays and processing methodologies. The results of the SPAC analysis are expressed in terms of phase velocity and frequency, instead of autocorrelation curves. This approach allows a direct comparison between SPAC and the other analyses conducted in this investigation, nevertheless empirical autocorrelation curves were introduced directly to the inversion process.

### 3.1 Results obtained with a high-energy active source

Figure 3 displays the amplitude of the Fourier spectrum computed at different distances from the shot position with a 100 kg weight, 3 m-drop (high-energy source), 18 lb sledgehammer (low-energy source) and ambient vibrations record in case 01. The frequency range and amplitudes of the shot generated by the high-energy source are larger than those generated by low-energy sources. The amplitudes developed with high-energy sources are approximately five times the amplitudes developed by the sledgehammer. Indeed, the high-energy source introduces an important amount of energy between 5 and 55 Hz approximately. The sledgehammer concentrates the energy between 8 and 60 Hz approximately. Outside these limits, their amplitudes are close to ambient vibrations amplitudes. These differences are reflected in the frequency ranges of the dispersion curves (Fig. 4). The high-energy source determines dispersion curves down to 5 Hz approximately, while the low-energy source is restricted to higher frequencies (larger than 7 Hz).

Similar results using a high-energy active source are also obtained for cases 02 and 03 (Table 1) as shown in Fig. 5. Results obtained with high-energy active sources are highly reliable for evaluating the dispersion curve for a wide range of frequencies. However, the aim of this investigation is to determine a methodology to seismically characterize soils using standard equipment. Therefore, the results obtained with high-energy sources will be used as a reference to validate results obtained with commercial equipment which is able to be used in urban environments.

The $V_S$ profiles obtained with the 100 kg weight, 3 m-drop are shown in Fig. 6. Only the profiles whose misfits are less than 1.5 times the minimum misfit are plotted. The inversion

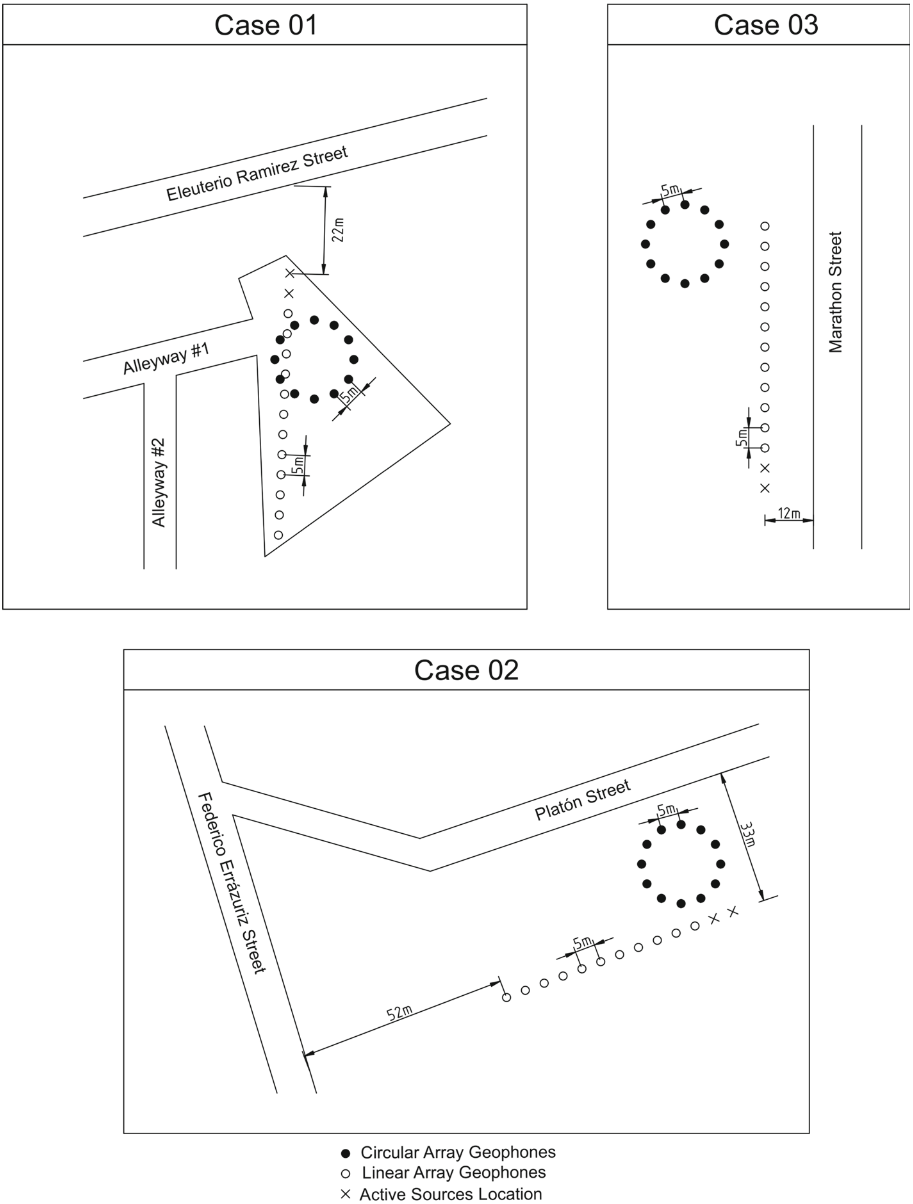


**Fig. 1** Location of arrays in the cases studied. Streets located within 100 m are included in each map

results are reliable up to a given depth, where there is a large dispersion of $V_S$ model values for the set that was evaluated. As shown in Fig. 6, in all three cases, the exploration is reliable at least until 30 m deep. Also, the stratigraphic information of each site is plotted in the same figure. For case 01, the results of boreholes available for this site (Seremi Metropolitana MINVU 2012a,b) indicate a soil structure mainly composed by clays, sandy silts, and loose sands up to a depth of 18 m. At this depth, the soil is mainly composed of dense and silty

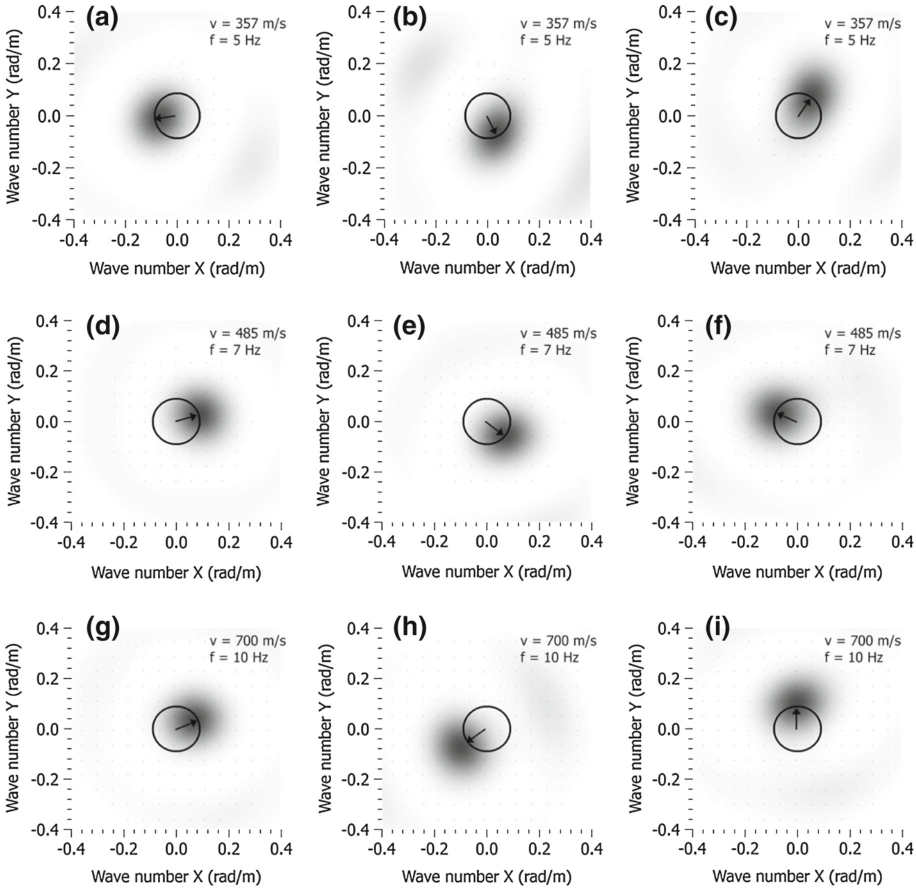


**Fig. 2** Representations of energy distribution in the $k_x - k_y$ wavenumber space for selected frequencies (f) and phase velocities (v): **a** case 01, **b** case 02 and **c** case 03. The *black arrow* indicates the angle of incidence of the passive source

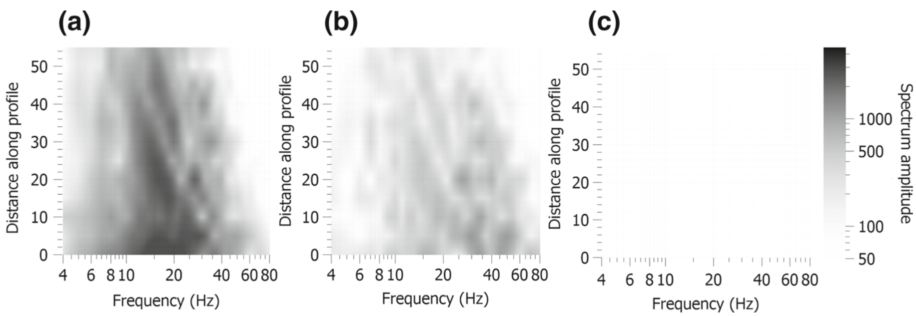


**Fig. 3** Amplitude spectrum obtained with **a** high-energy active source, **b** low-energy active source and **c** ambient vibrations in case 01

sands. Also, a thin layer of gravel is found between depths of 24–28 m. In case 02, the result of the available borehole in this site (Seremi Metropolitana MINVU 2012a,b) indicates a soil structure mainly composed of volcanic ashes (ignimbrite) with the presence of gravels

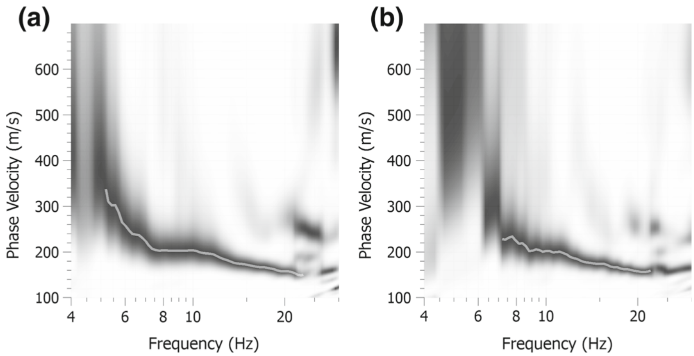


**Fig. 4** Dispersion curve obtained in active test using **a** high-energy and **b** low-energy sources in case 01

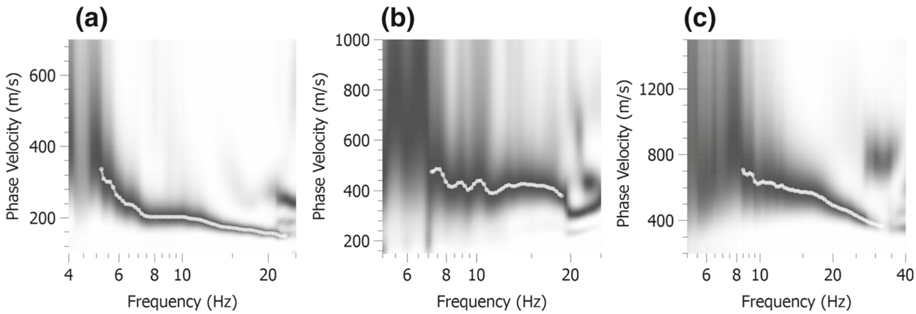


**Fig. 5** Dispersion curve obtained with 100 kg weight 3 m-drop in **a** case 01, **b** case 02, **c** case 03

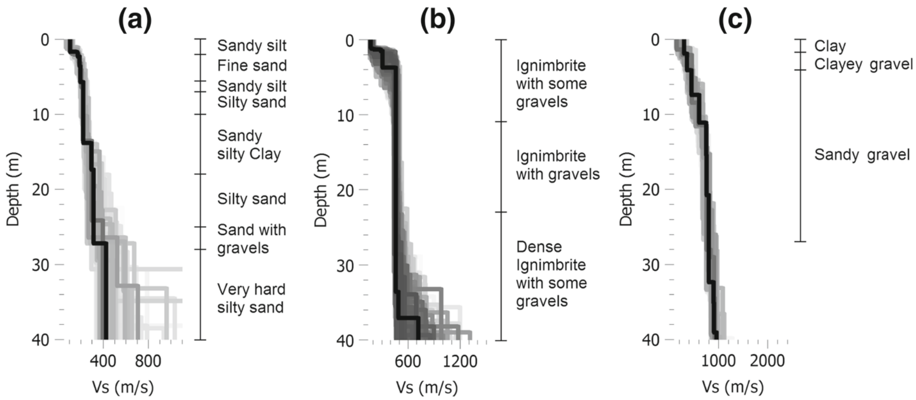


**Fig. 6** Shear wave velocities obtained with 100 kg weight 3 m-drop: **a** case 01, **b** case 02, and **c** case 03

beyond a depth of 11 m. Case 03 is placed in the San Joaquin Campus of Pontificia Universidad Católica de Chile. Based on multiple boreholes (Ampuero and Van Sint Jan 2004), the stratigraphy in the campus can be described as a very shallow clay layer followed by a clayey gravel layer (with a maximum depth of 4 m) and a wider layer mainly composed of sandy gravels until the maximum depth of exploration (27 m approximately). It is important to emphasize that the inversion process was conducted without incorporating borehole infor-

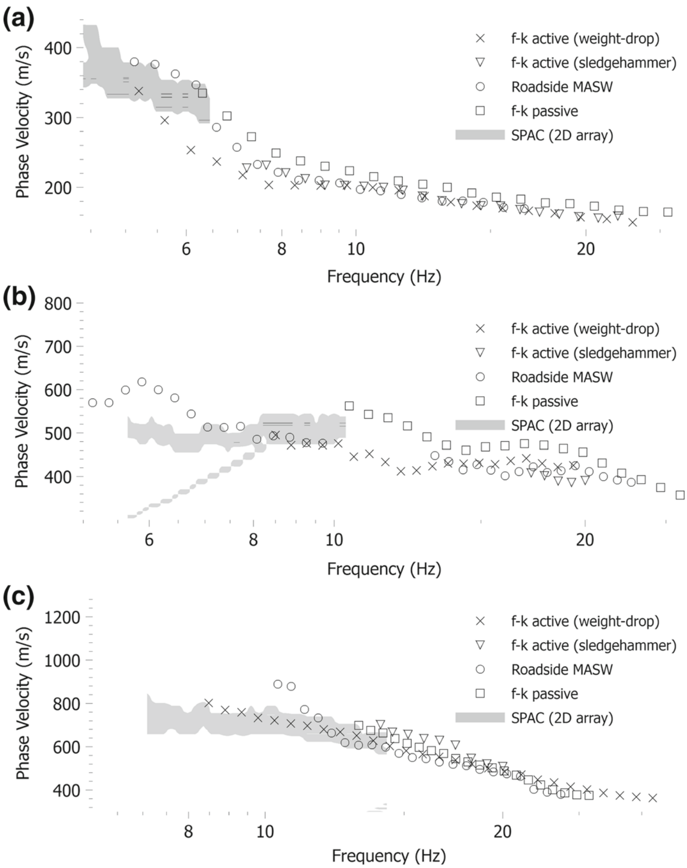


**Fig. 7** Dispersion curves obtained through different methodologies: **a** case 01, **b** case 02 and **c** case 03

mation. In addition, $V_S$ profiles are consistent with stratigraphy. These results will be used as a reference to compare results obtained with standard equipment.

## 3.2 Dispersive characteristics of the three selected cases

Figure 7 shows the dispersion curves obtained in active tests using both sources (f-k analysis), in passive tests using linear arrays (Roadside MASW analysis), and in passive tests using circular array (f-k and SPAC analysis).

In case 01 (Fig. 7a), the frequency ranges of dispersion curves obtained for this case are very similar among them. Active tests with sledgehammers allow accessing frequencies close to 7 Hz in comparison to 5 Hz reached using 100 kg weight 3 m-drop. The curves obtained in passive tests using linear and circular array are defined for frequencies over 5 and 6 Hz respectively, and both tend to over-predict phase velocities for frequencies below 7 Hz in comparison to velocities obtained with weight drop. Circular SPAC results define the dispersion curve for frequencies below 6.5 Hz, becoming an excellent complement to dispersion curves obtained using f-k analysis on linear and circular arrays. It’s important to note that changing the analysis method (from SPAC to f-k), enables the access to lower frequencies, using the same array and exactly the same data.

For case 02 (Fig. 7b), the dispersion curves obtained present several differences among them in comparison to case 01. The result given by an active test using a sledgehammer is discarded because the frequency range successfully explored is very low compared to other tests. The curves obtained in passive tests using linear arrays tends to predict large phase velocities for frequencies below 8 Hz in comparison to SPAC results, and present a diffuse concentration of energy between 10 and 13 Hz, making it impossible to identify the dispersion curve for that frequency range. Above 13 Hz, the dispersion curve obtained with a passive linear test is consistent with weight drop. The curves obtained with circular array have higher values of phase velocity for almost all frequencies compared to weight drop. This difference is probably related to the presence of lateral variation of soil properties. The differences are higher between 10 and 14 Hz and are probably related to a lack of resolution for that frequency range in the f-k analysis.

Finally, in case 03 (Fig. 7c) the dispersion curves obtained have different frequency ranges depending on the selected method. In the active test with sledgehammer and f-k analysis over circular array, the lowest frequency reached is around 14 Hz. This value is insufficient to explore the required 30 m. Smaller frequencies are successfully explored with the linear passive test and the SPAC analysis over the circular array. When compared to case 01, here the differences were greater between the results using f-k and SPAC analysis for the same circular array. Furthermore, the curve obtained with a SPAC analysis over circular array show similar phase velocities in low frequency ranges (between 8 and 14 Hz approximately) in comparison to weight drop results. For linear passive tests, phase velocity values are lightly over-predicted below 12 Hz, in comparison to weight drop results.

According to Chávez-García et al. (2005), it is possible to replace the azimuthal average required by the SPAC method with a temporal average resulting from a long time recording. This idea makes it possible to apply the SPAC method over linear arrays. In this research, the SPAC method was applied to same passive records analyzed with the Roadside MASW method and their results are shown in Fig. 8. As shown in Figs. 7 and 8, the identification of the dispersion curve in the SPAC results is less evident using linear arrays than circular arrays. Despite this fact, the results are satisfactory in the three considered cases in comparison to weight drop results. In case 01 (Fig. 8a) the dispersion curve is well defined between 5 and 6.5 Hz approximately and is consistent with the other curves obtained. In case 02 (Fig. 8b) the frequency range is wider (5–11 Hz) and is consistent with results obtained in active and passive linear tests. Finally, in case 03 (Fig. 8c), it is possible to identify, between 8 and 16 Hz, a dispersion curve in agreement with those obtained in active tests and SPAC analyses using circular array (Fig. 7c).

### 3.3 Shear wave velocity profiles obtained through an inversion process

Unlike 100 kg weight 3 m-drop results, the major part of the dispersion curves presented in the previous section show, by themselves, an insufficient amount of information to accurately reach the 30 m depth. A direct solution is to combine them in order to improve the inversion result. The frequency range can be extended combining active and passive results because the passive tests provide information for low frequencies, while the active tests are most efficient for high frequencies. Additionally, the use of SPAC results can also expand the frequency range. It is important to note that the dispersion curves displayed in Figs. 7 and 8 from SPAC analysis have been used only to define the frequency range where the information is reliable. However, it is more accurate to use the autocorrelation curves in the inversion process. Indeed, the Geopsy package allows directly using autocorrelation curves as a target for the inversion process. Nevertheless, results of the SPAC method explore the dispersive properties for a

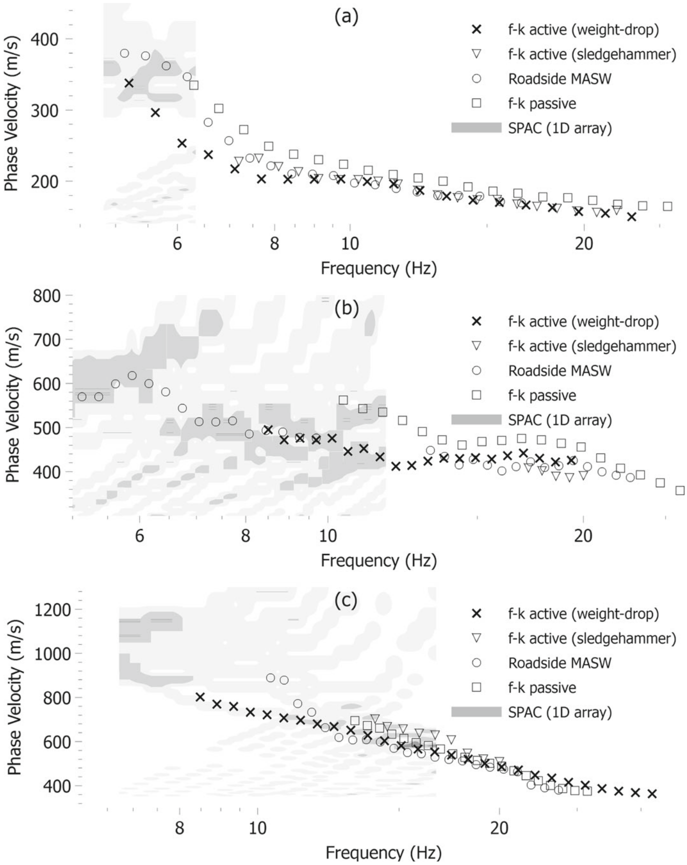


**Fig. 8** Dispersion curves obtained through different methodologies: **a** case 01, **b** case 02 and **c** case 03

bounded range of frequencies, thus the use of other dispersion or autocorrelation curves (e.g., from active experiments) is mandatory.

Poisson ratio and density were fixed for all layers with the same values for weight drop results. Any additional data was a variable for the inversion process. The combinations of data used in the inversion process are the following:

- LPA (Linear Passive and Active low energy tests): Combination of curves obtained in passive test by linear arrays (with Roadside MASW) and active test using 18 lb sledgehammer.
- LP (Linear Passive test): Only dispersion curve obtained in passive test by linear arrays with Roadside MASW.
- LCPA (Linear and Circular Passive, and Active low energy test): Combination of curves from active test using sledgehammer and passive test with linear (Roadside MASW) and circular arrays (f-k and SPAC).
- LPA2 (Linear Passive and Active low energy tests, including SPAC analysis): Combination of curves obtained in passive test by linear arrays (with Roadside MASW and SPAC) and active experiments using sledgehammer.

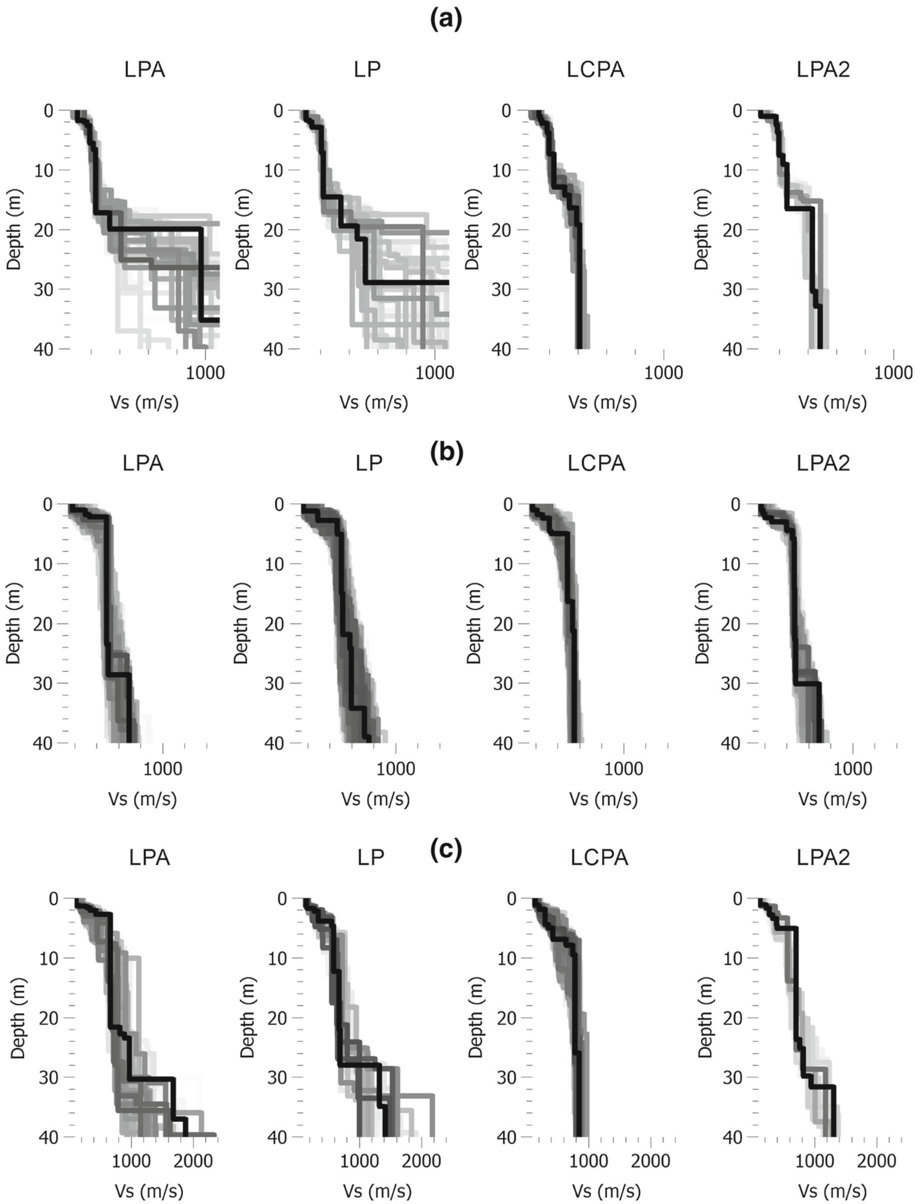


**Fig. 9** Shear wave velocities obtained through different inversion procedures: **a** case 01, **b** case 02, and **c** case 03

Currently, LP and LPA are the methods most frequently used currently in Chile. For each studied combination, the results are displayed in Fig. 9. In the same way as the 100 kg weight 3 m-drop results, only the profiles whose misfits are less than 1.5 times the minimum misfit are plotted. Also the inversion process was conducted blindly without incorporating borehole information. Results obtained through SPAC analysis over circular and linear arrays (LCPA and LPA2) produce a family of models which are consistent among them and with the known

**Table 2** Minimum misfit reached at each inversion process

| Case | AH | LPA | LP | LCPA | LPA2 |
|---|---|---|---|---|---|
| 01 | 0.0259 | 0.0284 | 0.0256 | 0.0784 | 0.1179 |
| 02 | 0.0379 | 0.0320 | 0.0297 | 0.0434 | 0.1169 |
| 03 | 0.0200 | 0.0558 | 0.0391 | 0.0619 | 0.1675 |

stratigraphy up 30 m depth. Also, in cases 01 and 03, the velocities in the deeper layers are below those obtained using the Roadside MASW method (inversion LPA and LP). It is because the dispersion curve obtained in the passive linear test systematically overestimates the velocities for low frequencies (as shown in Figs. 7, 8). The minimum misfit reached at each inversion process is reported in Table 2. It is important to note that misfit values increase if the inversion included SPAC results because the autocorrelation curve has an associated standard deviation appearing in the denominator of the misfit expression (1). The SPAC results are more reliable (because they incorporate more information), although the misfit increases.

In Fig. 10 the obtained $V_S$ profiles obtained with standard equipment are compared to profiles obtained by other methods. First, the results are compared to $V_S$ profiles obtained

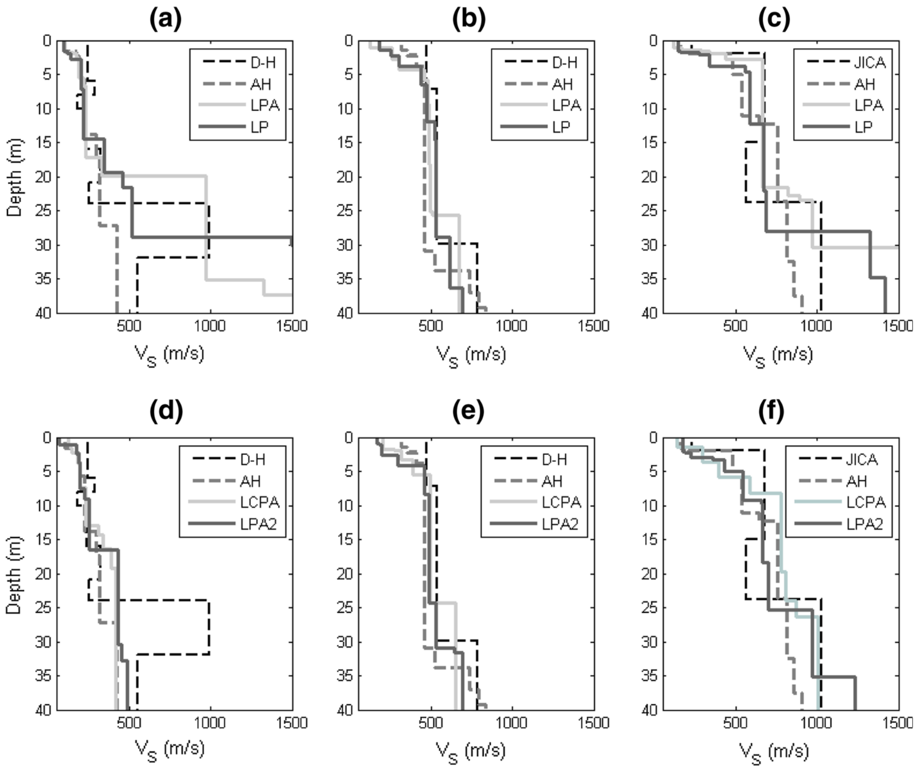


**Fig. 10** Comparison of shear wave velocity obtained through different inversion procedures with high-energy source (AH), down-hole (D-H) and obtained by JICA (Riddell et al. 1992): **a** and **d** case 01, **b** and **e** case 02, and **c** and **f** case 03

with high-energy source results (AH). Also, for cases 01 and 02, down-hole results are available (D-H), and for case 03, results from previous research are available. Riddell et al. (1992) conducted studies in order to geotechnically classify sites where some accelerometer stations were located (one of them is located in San Joaquin Campus), as part of a project with the Japan International Cooperation Agency (JICA). Tests were performed with large arrays of geophones using microvibrations measurements. These profiles were determined through SPAC method using a least-squares criterion for inversion (Tokimatsu 1992).

In case 01, down-hole results indicate the presence of a thin layer of gravel that is not identified by any inversion. The result of inversions LCPA and LPA2 are consistent with AH and D-H results, without considering the rigid thin layer detected in down-hole results. Inversions LPA and LP are consistent, just until 20 m deep, with AH and D-H results. In case 02, the four profiles obtained through the inversion process are very consistent with D-H and AH results. The big difference is that down-hole indicates the velocities in shallow layers (first 5 m) are above than 400 m/s, while velocities obtained though the inversion process are much lower. Finally, in case 03, the four methodologies seem to be consistent with results obtained by JICA and AH. Nevertheless, the results obtained using linear passive dispersion curves to explore low frequencies (LPA and LP) tends to increase the velocities for layers deeper than 30 m deep.

## 4 Proposed methodology for $V_{S,30}$ estimation

In Chile, the current soil classification is based on $V_{S,30}$ and an additional static parameter (e.g., corrected SPT blow count) (NCh 433, mod DS 61 2011). As a complete seismic classification requires these both values, in this article the authors have chosen lowercase letters to distinguish the soil classification from the official one. Table 3 provides the values for the proposed classifications, considering only the information provided by the geophysical tests.

Tables 4, 5 and 6 summarize $V_{S,30}$ obtained for each studied site with different inversion procedures (using the acronym to denote each inversion type as described in Sect. 3.2). Each inversion process generated 5,100 models with different misfit values. Some of these models have similar dispersive properties that were obtained empirically. In practical terms, even if these models have differences, they are equivalent according to their misfit reached. We fixed an arbitrary criterion to group those with similar dispersive properties. For each inversion process, 1 % of valid models with the lowest misfit value are considered as similar. These sets of similar solutions are useful to estimate $V_{S,30}$ uncertainties through some statistical parameters. So, for each set of similar profiles, we calculate the $V_{S,30}$ mean ($V_{S,30}$) and its coefficient of variation (CoV). The $V_{S,30}$ value of the smallest misfit profile and the CoV of $V_S$ at 30 m are also indicated in these tables.

**Table 3** Seismic classification according to $V_S$ results (NCh 433, mod DS 61 2011)

| Soil class | $V_{S,30}$ (m/s) |
|---|---|
| A | $900 \leq V_{S,30}$ |
| B | $500 \leq V_{S,30} < 900$ |
| C | $350 \leq V_{S,30} < 500$ |
| D | $180 \leq V_{S,30} < 350$ |
| E | $V_{S,30} < 180$ |

**Table 4** $V_{S,30}$ results with different inversion procedures in case 01

| | Number of similar profiles | Mean of similar profiles | | $V_{S,30}$ (m/s) of smallest misfit profile | Coefficient of variation of $V_S$ at 30 m |
|---|---|---|---|---|---|
| | | $V_{S,30}$ (m/s) | Coefficient of variation | | |
| AH | 51 | 258 | 0.12 | 244 | 0.18 |
| LPA | 51 | 297 | 0.17 | 279 | 0.40 |
| LP | 51 | 294 | 0.19 | 261 | 0.41 |
| LCPA | 51 | 276 | 0.09 | 269 | 0.04 |
| LPA2 | 51 | 278 | 0.13 | 257 | 0.13 |
| D-H | – | – | – | 299 | – |

**Table 5** $V_{S,30}$ results with different inversion procedures in case 02

| | Number of similar profiles | Mean of similar profiles | | $V_{S,30}$ (m/s) of smallest misfit profile | Coefficient of variation of $V_S$ at 30 m |
|---|---|---|---|---|---|
| | | $V_{S,30}$ (m/s) | Coefficient of variation | | |
| AH | 51 | 420 | 0.05 | 417 | 0.05 |
| LPA | 51 | 460 | 0.09 | 462 | 0.09 |
| LP | 51 | 474 | 0.09 | 468 | 0.08 |
| LCPA | 51 | 454 | 0.07 | 442 | 0.02 |
| LPA2 | 51 | 437 | 0.08 | 412 | 0.09 |
| D-H | – | – | – | 519 | – |

**Table 6** $V_{S,30}$ results with different inversion procedures in case 03

| | Number of similar profiles | Mean of similar profiles | | $V_{S,30}$ (m/s) of smallest misfit profile | Coefficient of variation of $V_S$ at 30 m |
|---|---|---|---|---|---|
| | | $V_{S,30}$ (m/s) | Coefficient of variation | | |
| AH | 51 | 599 | 0.12 | 555 | 0.05 |
| LPA | 51 | 602 | 0.19 | 573 | 0.16 |
| LP | 51 | 581 | 0.17 | 524 | 0.22 |
| LCPA | 102 | 594 | 0.14 | 552 | 0.03 |
| LPA2 | 77 | 593 | 0.18 | 527 | 0.15 |
| JICA | – | – | – | 608 | – |

Results obtained with LCPA are similar to those obtained with AH. Even better results are achieved with LCPA in case 01. LPA2 results are consistent with LCPA but slightly higher values of $V_S$ are obtained at 30 m. On the other hand, the inversion using just the passive linear curves (LP) tends to predict larger velocities in the deeper layers, while velocities of shallow layers tend to be lower. The combination of these effects explains why the mean value of $V_{S,30}$ obtained with LP in case 03 is similar to that obtained with AH and LCPA. Also larger differences are shown for $V_S$ at 30 m in case 01. Combining active and passive linear dispersion curves to obtain more information in high frequencies tends to increase velocities in the shallow layers (similar values from inversions AH and LCPA) but with higher values in the deeper layers. For that reason LPA results are larger than those with LP in case 01.

$V_S$ profiles obtained with LPA and LP are similar in cases 02 and 03. This occurs because the frequency range included by the active test using a sledgehammer does not contribute to extend the frequency range of linear passive test. So the calculated $V_{S,30}$ depends on the overestimated velocities assumed in deeper layers. The best result observed with LP, LPA and LPA2 methodologies occurs when there is a street perpendicular to the linear array (Case 02).

Down-hole results are higher in all cases, even changing the seismic soil classification according to Table 3 (case 02). It can be explained by the differences observed in shallow layers where D-H profiles show high velocities. The trend shown by surface wave methods is more realistic at shallow layers where there is a strong influence of lateral confinement.

Each inversion procedure combination provides very similar CoV values for each site; these results are consistent with conclusions reported by Comina et al. (2011) confirming that the inversion non-uniqueness does not significantly alter the reliability of the $V_{S,30}$ estimate. The smaller CoV value was obtained using combinations of AH and LCPA for each case; LCPA has the advantage of being performed with standard equipment.

According to $V_S$ profiles obtained and $V_{S,30}$ calculated, the LCPA procedure is able to classify soils for the first 30 m depth. In case 03 the coefficient of variation of $V_S$ reached at 30 m deep with LPA2 indicated that this procedure doesn't guarantee a reliable exploration. Indeed, the experiments of Chávez-García et al. (2006) were performed without high-traffic roads in the proximity. To validate the performance of this strategy, it is mandatory to investigate some other conditions regarding ambient noise.

## 5 Performance of inversion procedures with standard equipment

Procedures LCPA and LPA2 correspond to experiments that can be performed with "standard" equipment, without sophisticated controlled source devices. In order to study their performance, two factors will be analyzed: high-traffic road proximity and differences observed depending on the orientation of linear arrays related to predominant ambient noise source.

To study the influence of a road or street close to the array, 20 additional cases (all of them in the Santiago metropolitan area) were analyzed and their results are summarized in Table 7. In these cases, $V_{S,30}$ were obtained using procedures LPA, LP, LCPA and LPA2. The purpose of including LPA and LP, is to observe their performance alongside a road (implicit assumption when Roadside MASW method is applied; Park and Miller 2001), especially in cases with high traffic of vehicles. In all cases, the active source used was an 18 lb sledgehammer.

The main differences observed for procedures LPA and LP with respect to LCPA are related to proximity to a high-traffic road. In low traffic conditions, differences between LPA and LCPA are close to 17 %, while between LP and LCPA the difference is close to 24 %. On the other hand, in high traffic conditions, these differences are close to 12 and 16 %, respectively. In general terms, the results obtained with LPA2 seem to be independent of the traffic condition. Also, the difference on $V_{S,30}$ calculated with LCPA and LPA2 is smaller than other cases.

The cases A07, A19 and A20 show the most significant differences among procedure LCPA and procedures LPA and LP. As shown in Fig. 11, there are large differences in $V_S$ estimated for deeper layers in these cases. It was the same phenomenon observed on case 01 in Sect. 3, where the Roadside MASW method tends to over-predict values in deeper layers in comparison to velocities obtained with LCPA methodology.

**Table 7** Performance of methodologies bases on linear array for passive measurements (inversion LPA, LP and LPA2) in comparison to methodology based on 2D array for passive measurements to $V_{S,30}$ estimation (LCPA)

| Case | Orientation[a] | Traffic[b] | $V_{S,30}$ (m/s) | | | | Difference between LCPA and | | |
|---|---|---|---|---|---|---|---|---|---|
| | | | LPA | LP | LCPA | LPA2 | LPA (%) | LP (%) | LPA2 (%) |
| A01 | Non oriented | LT | 329 | 329 | 352 | 343 | −6.5 | −6.5 | −2.6 |
| A02 | Perpendicular | LT | 242 | 261 | 243 | 240 | −0.4 | 7.4 | −1.2 |
| A03 | Perpendicular | HT | 254 | 234 | 255 | 249 | −0.4 | −8.2 | −2.4 |
| A04 | Perpendicular | HT | 287 | 276 | 294 | 305 | −2.4 | −6.1 | 3.7 |
| A05 | Perpendicular | HT | 495 | 516 | 534 | 494 | −7.3 | −3.4 | −7.5 |
| A06 | Perpendicular | HT | 332 | 382 | 345 | 379 | −3.8 | 10.7 | 9.9 |
| A07 | Perpendicular | HT | 471 | 488 | 421 | 458 | *11.9* | *15.9* | *8.8* |
| A08 | Perpendicular | HT | 425 | 402 | 400 | 404 | 6.3 | 0.5 | 1.0 |
| A09 | Perpendicular | HT | 446 | 416 | 429 | 464 | 4.0 | −3.0 | 8.2 |
| A10 | Perpendicular | LT | 512 | 513 | 509 | 528 | 0.6 | 0.8 | 3.7 |
| A11 | Perpendicular | LT | 533 | 530 | 508 | 533 | 4.9 | 4.3 | 4.9 |
| A12 | Perpendicular | LT | 439 | 441 | 427 | 431 | 2.8 | 3.3 | 0.9 |
| A13 | Parallel | HT | 418 | 409 | 408 | 414 | 2.5 | 0.2 | 1.5 |
| A14 | Parallel | HT | 303 | 306 | 296 | 317 | 2.4 | 3.4 | 7.1 |
| A15 | Parallel | HT | 431 | 372 | 411 | 442 | 4.9 | −9.5 | 7.5 |
| A16 | Parallel | HT | 572 | 564 | 561 | 592 | 2.0 | 0.5 | 5.5 |
| A17 | Parallel | LT | 315 | 320 | 317 | 299 | −0.6 | 0.9 | −5.7 |
| A18 | Parallel | LT | 261 | 275 | 258 | 259 | 1.2 | 6.6 | 0.4 |
| A19 | Parallel | LT | 336 | 345 | 307 | 309 | 9.4 | 12.4 | 0.7 |
| A20 | Parallel | LT | 440 | 464 | 374 | 420 | *17.6* | *24.1* | *12.3* |

The performance is evaluated for different traffic conditions, orientations respect of closest road or street and soil class

[a] Orientation of linear array respect of closest road or street

[b] High traffic means that case studied is placed near roads or high traffic avenues, while low traffic means the case is placed far from roads or high-traffic avenues

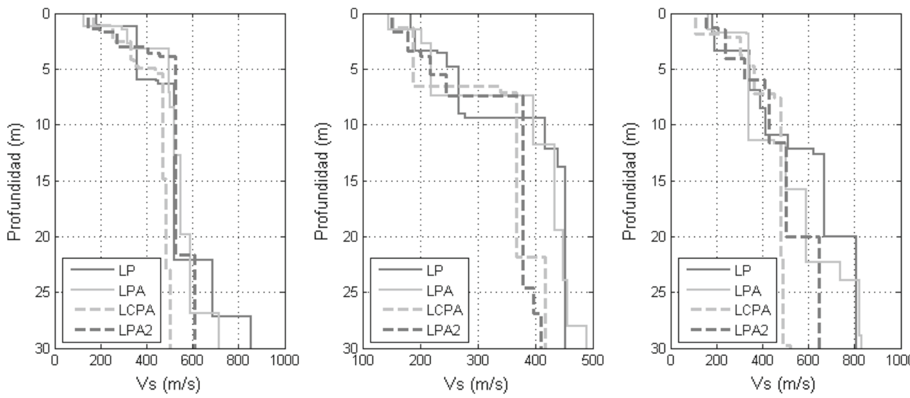


**Fig. 11** Cases from Table 6 whose shear wave velocity profiles present strong differences among inversion LPA or LP with inversion LCPA: case A07, case A19, case A20

However, the results obtained with LPA2 for case A19 are similar to those observed with LCPA. This doesn't occur for cases A07 and A20, where high differences can be noticed (in italics in Table 7). For this reason, a seismic classification cannot be based only on LPA2 results. For future investigations, we recommend reviewing more cases to generalize the performance of LPA2, especially in volcanic ash deposits (Gálvez 2012), where four of the five cases with the higher differences between LCPA and LPA2 methodologies are located.

It is important to note that in some cases (A01, A05 and A06), $V_{S,30}$ obtained using different methodologies implies a change in the seismic classification. According to obtained results, in cases when the seismic classification is 10 % above the limit between two seismic classes (Table 2), it is recommendable to check the seismic class assigned that was obtained with two different methodologies, including a 2D analysis.

## 6 Conclusions

To ensure a reliable exploration of the first 30 m of soils, it is necessary to determine dispersive properties for a wide range of frequencies (5–20 Hz in soft soils and 10–30 Hz in rigid soils). To achieve appropriate results using standard equipment, it is necessary to combine dispersion curves obtained with standard-energy source and data from different passive methods over linear and circular arrays. In the case of passive linear tests, high traffic proximity is an important factor (e.g., procedures based only on the Roadside MASW method), but it can be mitigated including SPAC analysis.

According to the results of this investigation, the following methodologies are proposed:

1. Use a high-energy active source able to explore the 30 m.
2. Combine active source with a sledgehammer and ambient vibrations recorded by linear (Roadside MASW and SPAC) and 2D arrays (f-k and SPAC), to evaluate the performance of the inversion process for different combinations of data. The array used in this research (9.8 m radius circle) demonstrated its ability to explore the 30 m required just using SPAC analysis for all soil classes defined in the Chilean seismic code. Additionally, its size is appropriate to be used in urban areas.

In most cases, the dispersion curves obtained in passive tests using linear arrays, and only Roadside MASW analysis, satisfactorily describes a limited frequency range, which does not allow a reliable exploration of the first 30 m of depth. Therefore, a methodology based only on the inversion of the curve obtained in a passive test using linear arrays is not recommendable. In the same way, a methodology based on the combination of a dispersion curve obtained in active and linear passive tests does not guarantee the usually required 30 m of exploration. According to the results of this investigation, it is especially complex for cases when there are no high traffic roads or streets close to the explored site. For that reason, care is advised in the use of this methodology, ensuring that it effectively explores the deeper layers without an overestimation of their velocities that can lead to a wrong seismic site classification.

**Acknowledgments** This research was partially supported by a grant from the Chilean National Commission for Scientific and Technological Research, under the National Research Center for Integrated Natural Disaster Management CONICYT/FONDAP/15110017 and partially by Geofísica TRV. We thank Mr. Tony Rojas and Geofísica TRV team for the support during the fieldwork campaigns and for lending their 100 kg weight 3 m-drop seismic source; we also thank the undergraduate-students who actively participated in field campaigns at different stages of this investigation.

## References

Aki K (1957) Space and time spectra of stationary stochastic waves, with special reference to microtremors. Bull Earthq Res Inst 35:415–456

Ampuero A, Van Sint Jan M (2004) Velocidades de onda medidas en Santiago con el ensayo de refracción sísmica. In: V Congreso Chileno de Ingeniería Geotécnica, Santiago, Chile

Bettig B, Bard P, Scherbaum F, Riepl J, Cotton F, Cornou C, Hatzfeld D (2001) Analysis of dense array noise measurements using the modified spatial auto-correlation method (SPAC): application to the Grenoble area. Bolletino di Geofisica Teorica ed Applicata 42:281–304

Bonnefoy-Claudet S, Baize S, Bonilla L, Berge-Thierry C, Pasten C, Campos J, Volant P, Verdugo R (2009) Site effect evaluation in the basin of Santiago de Chile using ambient noise measurements. Geophys J Int 176:925–937

Chávez-García F, Rodríguez M, Stephenson W (2005) An alternative approach to the SPAC analysis of microtremors: exploiting stationarity of noise. Bull Seismol Soc Am 95:277–293

Chávez-García F, Rodríguez M, Stephenson W (2006) Subsoil structure using SPAC measurements along a line. Bull Seismol Soc Am 96:729–736

Comina F, Foti S, Boiero D, Socco LV (2011) Reliability of VS,30 evaluation from surface-wave tests. J Geotech Geoenviron Eng 137:579–586

Foti S (2000) Multistation methods for geotechnical characterization using surface waves. Ph.D. thesis, Politecnico di Torino

Foti S, Lancellota R, Socco LV, Sambuelli L (2001) Application of FK analysis of surface waves for geotechnical characterization. In: Proceedings of the fourth international conference on recent advances in geotechnical earthquake engineering and soil dynamics and symposium in honour of professor W.D. Liam Finn; March 26–31, 200, San Diego, California. Paper No. 1.14, 6 pp

Gálvez C (2012) Microzonificación sísmica en los sectores de Lampa y Batuco, Región Metropolitana. Chile. Memoria para optar al título de Geólogo. Universidad de Chile, Santiago, Chile

Nazarian S, Stokoe KH II (1984) In situ shear wave velocities from spectral analysis of surface waves. In: Proceedings of the 8th conference on earthquake engineering. Prentice-Hall, San Francisco, pp 31–38

Norma NCh 433 mod D.S. 61 (2011) Instituto Nacional de Normalización, Santiago, Chile

Okada H (2003) The microtremor survey method. Geophysical Monographs Series, no. 12. Society of Exploration Geophysicists

Park C, Miller R, Xia J (1998) Imaging dispersion curves of surface waves on multi-channel record. Society of Exploration Geophysicists Expanded Abstracts 1377–1380

Park C, Miller R, Xia J (1999) Multichannel analysis of surface waves. Geophysics 64:800–808

Park C, Miller R (2008) Roadside passive multichannel analysis of surface waves (MASW). J Environ Eng Geophys 13:1–11

Riddell R, Van Sint Jan M, RajMidorikawa S, Gajardo J (1992) Clasificación geotécnica de los sitios de estaciones acelerográficas en Chile. Departamento de Ingeniería Estructural y Geotécnica, Pontificia Universidad Católica de Chile, Santiago, Chile

Sambridge M (1999) Geophysical inversion with neighborhood algorithm—I. Searching the parameter space. Int Geophys J 138:479–494

Sanchez-Salinero I (1987) Analytical investigation of seismic methods used for engineering applications. Ph.D. dissertation. University of Texas at Austin

Seremi Metropolitana MINVU (2012a) Estudio de riesgo y modificación PRMS sector norte de Santiago, ID No 640-31-LP11, Informe Etapa 2, Prospecciones y Ensayes

Seremi Metropolitana MINVU (2012b) Estudio de riesgo y modificación PRMS sector poniente de Santiago, ID No 640-34-LP11, Informe Etapa 2, Prospecciones y Ensayes

Tokimatsu K (1992) Use of short-period microtremors for $V_S$ profiling. J Geotech Eng 118:1544–1558

Tokimatsu K (1997) Geotechnical site characterization using surface waves. In: Ishihara (ed) Balkema. Proceedings of the 1st international conference earthquake geotechnical engineering, pp 1333–1368

Wathelet M (2002–2011) GEOPSY packages (Version 2.5.0) [software]: retrieved from http://www.geopsy.org/download.php

Wathelet M (2005) Array recordings of ambient vibrations: surface-wave inversion. Ph.D. thesis. Université de Liège, Liège, Belgium

Wathelet M (2008) An improved neighborhood algorithm: parameter conditions and dynamic scaling. Geophys Res Lett 35:L09301. doi:10.1029/2008GL033256

Xia J, Miller RD, Park CB (1999) Estimation of near-surface shear-wave velocity by inversion of Rayleigh waves. Geophysics 64:691–700